Addition Spectra of Chaotic Quantum Dots: Interplay between Interactions and Geometry

Kang-Hun Ahn,[1] Klaus Richter,[1] and In-Ho Lee[2]
[1]*Max-Planck-Institut für Physik komplexer Systeme, Nöthnitzer Strasse 38, 01187 Dresden, Germany*
[2]*School of Physics, Korea Institute for Advanced Study, Cheongryangri-dong, Seoul 130-012, Korea*
(Received 2 June 1999)

We investigate the influence of interactions and geometry on ground states of clean chaotic quantum dots using the self-consistent Hartree-Fock method. We find two distinct regimes of interaction strength: While capacitive energy fluctuations $\delta\chi$ follow approximately a random matrix prediction for weak interactions, there is a crossover to a regime where $\delta\chi$ is strongly enhanced and scales roughly with interaction strength. This enhancement is related to the rearrangement of charges into ordered states near the quantum dot edge. This effect is nonuniversal depending on the shape and the size of the dot. It may provide insight into recent experiments on statistics of Coulomb blockade peak spacings.

PACS numbers: 72.10.Fk, 05.45.–a, 73.20.Dx

The understanding of the interplay between many-body interactions and chaos has evolved to a prominent field in mesoscopic physics. This challenging issue brings together two seemingly disconnected fields, namely many-particle physics and quantum chaos. Classically chaotic independent-particle dynamics is found in mesoscopics for both disordered systems due to scattering at impurities and *clean* quantum dots, where the shape of the confining potential can give rise to chaotic electron motion. While interaction effects in disordered systems have been intensively studied in the recent past [1], accounts on the interrelation between many-body effects and chaotic dynamics in ballistic quantum dots are still rare (see, e.g., Refs. [2,3]). The latter systems can be modeled by quantum billiards which have served as prototypes to investigate quantum signatures of integrable and chaotic single-particle dynamics [4]. Hence a generalization of these quantum chaos concepts to interacting particles in billiards appears natural. In this letter we approach this problem within a self-consistent Hartree-Fock (SCHF) approximation after checking its validity by comparing with exact diagonalization.

Our work was partly motivated by new measurements of charge transport through quantum dots with variable size and shape, which represent ideal tools to investigate experimentally the interaction effects in confined chaotic systems. If such a dot with N electrons and ground state energy E_N is only weakly coupled to external leads a conductance peak is observed, upon tuning a gate voltage connected to the dot, whenever the chemical potential $\mu_N = E_N - E_{N-1}$ coincides with that of the leads. In between the pronounced conductance peaks the current through the dot is suppressed due to Coulomb blockade [5]. The spacing between neighboring peaks as a function of gate voltage is proportional to the capacitive energy

$$\chi_N = E_{N+1} - 2E_N + E_{N-1}\,. \tag{1}$$

A number of recent experiments [6–9] showed that fluctuations of χ_N resemble a Gaussian distribution, while the assumption of a constant interaction (CI), which properly describes the mean peak spacing, combined with random matrix theory (RMT), predicts a Wigner-Dyson distribution. Two reasons have been proposed for the Gaussian distribution, the scrambling of the single-particle spectrum due to interactions [6,10–13] and the deformation of the dot by changing the gate voltage [14].

However, it is not yet understood why the measured peak spacing fluctuations, $\delta\chi = (\langle\chi_N^2\rangle - \langle\chi_N\rangle^2)^{1/2}$, significantly vary between the different experiments: Patel *et al.* [8] found rather small fluctuations which are comparable to the single-particle mean level spacing Δ. They are in line with the RMT + Cl model predicting $\delta\chi = \Delta(4/\pi - 1)^{1/2} \simeq 0.52\Delta$, and with RPA calculations for weak interactions (high densities, $r_s < 1$) [15,16]. However, the other experiments yield large fluctuations which scale with $\langle\chi_N\rangle$ rather than with Δ: $\delta\chi \approx 0.06 - 0.15\langle\chi_N\rangle$ in Refs. [6,7,9]. E.g., in a recent experiment [9], where the shape of the dot was not expected to be distorted by tuning the gate voltage, $\delta\chi$ was found to be 15 times larger than predicted by RMT.

Thus two main open questions arise: (i) What are the responsible mechanisms for the large fluctuations, and (ii) why do they show such a sample-dependent behavior, assuming that the samples are chaotic?

Here we consider clean chaotic quantum dots and study the interplay between the Coulomb interaction of the electrons and the geometry of the dots. We propose a mechanism for enhanced capacitive energy fluctuations $\delta\chi$ in chaotic structures and show that (i) interaction drives the systems to a regime of large, nonuniversal fluctuations by developing ordered charge states near the edges, and (ii) the shape of the confinement is an important factor for the formation of such states and hence for the fluctuations.

To our knowledge, all related theoretical studies consider interaction effects for disordered models [6,10–13], apart from the work by Stopa [2], who suggested the occurrence of strongly scarred states as a mechanism for enhanced fluctuations. Our calculations show that $\delta\chi$ can be enhanced in the absence of scarred states.

 0031-9007/99/83(20)/4144(4)$15.00

We model the quantum dots by a family of billiards that arises from a deformation of the disk [17]. The quantum billiards have already been employed as noninteracting models in the context of Coulomb blockade [14,18]. Here they will serve as appropriate tools to study interaction effects upon changing the billiard geometry. The confinement is defined by a hard-wall potential U satisfying $U(u,v) = 0$ inside a domain D and $U(u,v) = \infty$ outside. Using complex coordinates $\omega = u + iv$ and $z = x + iy$, D is defined by the conformal mapping [17] $\omega(z) = R(z + bz^2 + ce^{i\delta}z^3)/(\sqrt{1 + 2b^2 + 3c^2}); |z| < 1$. The real parameters b, c, and δ determine the shape, and R defines the dot size and area, $A = \pi R^2$. For the deformations to be considered (right insets of Fig. 2) the classical single-particle dynamics is predominantly chaotic (described by a large Kolmogorov entropy for the strongest deformation [18]), and we found that the single-particle energies exhibit Wigner-Dyson statistics.

To include interactions we first calculate the single-particle eigenfunctions ϕ_i and eigenenergies ϵ_i of a deformed billiard. We then use them to construct the Coulomb interaction matrix elements $V_{ijkl} = \int d\mathbf{r}_1\, d\mathbf{r}_2\, \phi_i(\mathbf{r}_1)\phi_j(\mathbf{r}_2)V(\mathbf{r}_1 - \mathbf{r}_2)\phi_k(\mathbf{r}_1)\phi_l(\mathbf{r}_2)$ with $V(\mathbf{r}) = e^2/\epsilon r$, and the many-electron Hamiltonian

$$H = \sum_i \epsilon_i c_i^\dagger c_i + \frac{1}{2}\sum_{ijkl} V_{ijkl} c_i^\dagger c_j^\dagger c_l c_k . \qquad (2)$$

Here $c_i^\dagger$ (c_i) creates (annihilates) the ith eigenstate of the noninteracting Hamiltonian. In terms of energy units $\hbar^2/(2m^*R^2)$, V_{ijkl} is proportional to the dimensionless interaction strength, or system size, R/a_B^*, where $a_B^* = \hbar^2\epsilon/m^*e^2$ is the effective Bohr radius. Equation (2) can serve as a starting point for both the exact diagonalization for few electrons [19] and SCHF calculations.

In this paper we focus on *ground state* properties for many-electron quantum dots and employ SCHF systematically for systems up to 27 spinless electrons. The SCHF allows us to calculate the ground state energies even in the presence of two-electron density correlations which are ignored in the RPA perturbation calculations [15,16]. To check the validity of our SCHF results for the capacitive energies χ_N, we first compare them with exact diagonalization results for few electrons. As shown in Fig. 1 the SCHF results are very accurate even for strong interactions.

The SCHF results for χ_N do not show any visible dependence on N but rather on the interaction strength (system size) R/a_B^*. Let us thus consider the mean fluctuations $\delta\chi$, where the statistical average $\langle\cdots\rangle$ is performed over N as in the experiments [6–9].

Our main results are summarized in Fig. 2. It shows $\delta\chi$ as a function of interaction strength for three different geometries depicted as insets close to the curves. For small size quantum dots, $R/a_B^* \lesssim 12$, $\delta\chi$ is close to the RMT prediction. Most interestingly, we find for larger

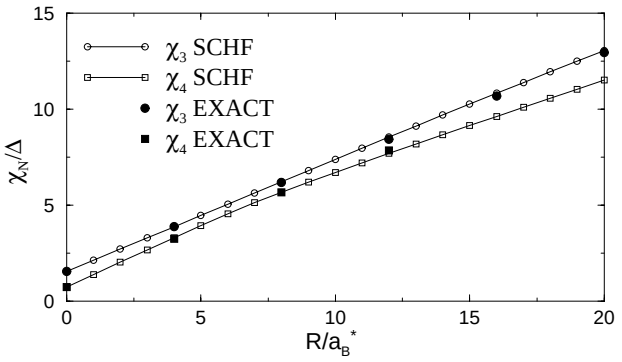

FIG. 1. Comparison of self-consistent Hartree-Fock (SCHF) and exact diagonalization (EXACT) results of capacitive energies χ_N [Eq. (1)] as a function of interaction strength for $N = 3$ (upper curve) and $N = 4$ (lower curve) for the billiard geometry shown in the bottom right inset of Fig. 2.

R/a_B^* a *crossover* to a regime where the capacitive energy fluctuations increase roughly linearly with increasing interaction strength. To our knowledge such clearcut crossover behavior has not been found in any tight-binding model for disordered systems. This indicates that it could be a property of the charge distribution in confined ballistic systems.

Using the standard definition of r_s, namely, $r_s^2 = A/(\pi N a_B^{*2})$, we have $r_s = (R/a_B^*)/\sqrt{N}$. Since we calculate $\delta\chi$ over a range $3 \le N \le 27$ for a given value of R/a_B^* in Fig. 2, r_s does not have a well-defined value but is in the range $(1/\sqrt{27})R/a_B^* \le r_s \le (1/\sqrt{3})R/a_B^*$. Hence the crossover value of R/a_B^* in Fig. 2 implies that

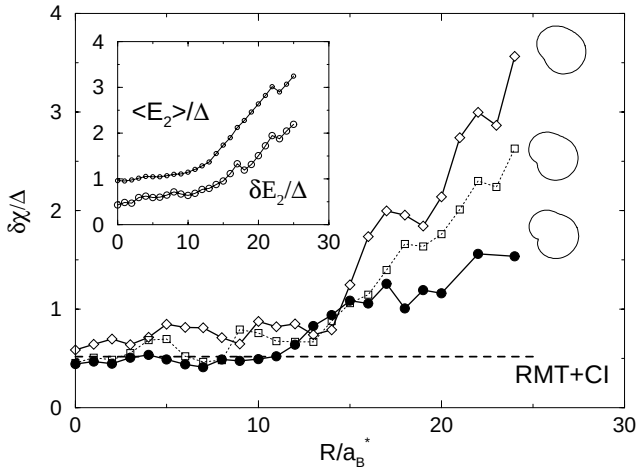

FIG. 2. Fluctuations of capacitive energies $\delta\chi = (\langle\chi_N^2\rangle - \langle\chi_N\rangle^2)^{1/2}$ as a function of interaction strength for interacting electrons in three chaotic billiards of different shapes shown on the right (defined with $\delta = 1.5$, $b = c = 0.12, 0.16$, and 0.2 from above, see text). $\delta\chi$ shows a clear crossover near $R/a_B^* = 12$ and increases with increasing R/a_B^* in the strong interaction regime. An analysis of the statistical error in computing $\delta\chi$ shows that it is of the order of the fluctuations visible in the curves. Inset: the mean and rms value of $E_2 = \epsilon_{N+2}^{(N)} - \epsilon_{N+1}^{(N)}$ for the quantum dot in the bottom right of the inset. Note that, for larger interactions, $\langle E_2\rangle \neq \Delta$.

$\delta\chi$ retains its RMT value up to $r_s \approx 2$ which is consistent with the RPA approach of Ref. [15].

In the following we discuss the mechanism responsible for the crossover to enhanced fluctuations $\delta\chi$. To this end it proves convenient to decompose χ_{N+1} as [15]

$$\chi_{N+1} \simeq [\epsilon_{N+2}^{(N+1)} - \epsilon_{N+2}^{(N)}] + [\epsilon_{N+2}^{(N)} - \epsilon_{N+1}^{(N)}] \equiv E_1 + E_2 . \quad (3)$$

Here, $\epsilon_j^{(i)}$ denotes the jth eigenvalue of the SCHF Hamiltonian with i electrons. Quantitatively, Eq. (3), which relies on Koopmans' approximation, does not give the same value as $\delta\chi$ in Fig. 2. However, Eq. (3) shows the same qualitative behavior with the same crossover point but slightly larger slope than in the SCHF case (Fig. 2).

The quantity E_1 in Eq. (3), which describes the interaction energy between the electrons in $(N+1)$th and $(N+2)$th states, has been considered in Ref. [15]. E_2 is the energy difference between two adjacent single-particle levels of the same Hamiltonian. In the RPA approach [15], it was claimed that $\langle E_2\rangle$ is given by Δ and its fluctuations δE_2 follow the RMT value $\simeq 0.52\Delta$. As displayed in the left inset of Fig. 2 our calculations show that this seems to be true for $R/a_B^* \lesssim 12$, which includes the regime $r_s < 1$, where RPA is reliable. However, $\langle E_2\rangle/\Delta$ grows as the system size increases, and $\delta E_2/\Delta$ and $\delta E_2/\langle E_2\rangle$ no longer follow the RMT prediction for $R/a_B^* \gtrsim 12$.

The similarity of the crossover behavior of $\delta\chi$ and δE_2 in Fig. 2 suggests that an analysis of E_2 proves appropriate to understand the enhanced fluctuations $\delta\chi$.

What happens in the regime $R/a_B^* \gtrsim 12$? To answer this question we present in Fig. 3 the evolution of unoccupied SCHF single-particle levels $\epsilon_n^{(N)}, n = N+1, N+2, \ldots$ with increasing interaction for a few representative values of N. We find that the enhancement of mean and rms values of $E_2 = (\epsilon_{N+2}^{(N)} - \epsilon_{N+1}^{(N)})$ is accompanied by the appearance of sudden jumps of the single-particle levels as marked by vertical arrows in Fig. 3. (Note, however, that the energy levels do not show for all values of N such jumps in the R/a_B^* range considered, e.g., $N = 16$.)

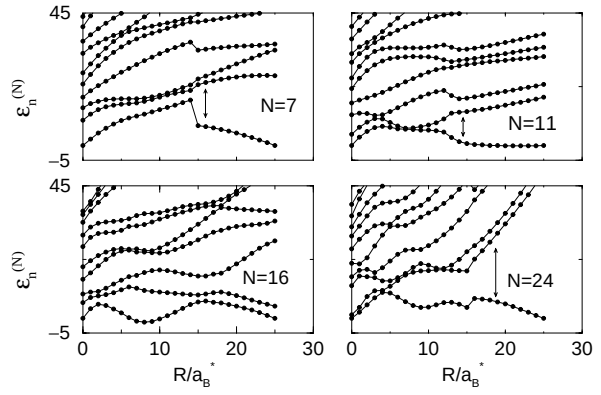

FIG. 3. Unoccupied SCHF levels $\epsilon_n^{(N)}$, $n = N+1, N+2, \ldots$, as a function of interaction strength for a chaotic quantum dot (bottom right of inset of Fig. 2) with $N = 7$, 11, 16, and 24 electrons. Note the sudden jumps in the level spacings E_2 between the lowest two adjacent levels which are caused by abrupt changes in the mean-field potential. For clarity, the levels in each panel are shifted by an amount $a(N) + b(N)R/a_B^*$. The energy units are $\hbar^2/2m^*R^2$.

The abrupt changes in the SCHF single-particle energies go along with a rearrangement of the corresponding wave functions, as shown in Figs. 4(a) and 4(b). This indicates a change in the total charge densities and thereby in the underlying mean-field potential. The two lower left (right) panels in Fig. 4 depict the total charge densities for interaction strength $R/a_B^* = 5$ (15) for two selected, representative N. A systematic analysis of a large number of geometries and particle numbers allowed us to extract two common trends visualized in the figure.

(i) With growing system size the electrons tend to be localized near the edge of the dot. *For $R/a_B^* \gtrsim 12$ the charges are reorganized in an ordered structure similar to a one-dimensional crystal or a charge-density-wave state.*

(ii) An abrupt change in the mean-field potential for fixed N occurs when an electron from the inner region of the dot moves into a state close to the edge.

Let us discuss the connection to the increase in $\langle E_2\rangle$ and δE_2. Electrons in states extending over the whole dot for small R/a_B^* move with increasing interaction to the edge due to the long-range Coulomb repulsion. When the states near the edge are fully occupied [see, e.g., Fig. 4(d)] the corresponding mean field reduces the accessible space for the next electron above the Fermi level [crossover from 4(a) to 4(b)]. The reduced effective size of the dot gives rise to an enhanced level spacing $\langle E_2\rangle$ which is accompanied by enhanced fluctuations.

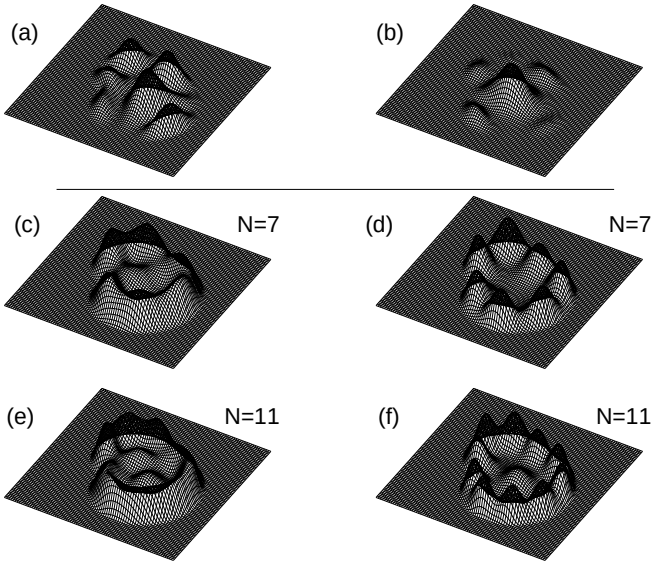

FIG. 4. Charge reordering with increasing interaction for a chaotic dot (bottom right inset of Fig. 2); $R/a_B^* = 5$ (15) in left (right) panels. Panels (a) and (b) show the probability density of the first unoccupied SCHF single-particle state $n = 8, N = 7$ (lowest curve in upper left panel, Fig. 3). In (c)–(f) the total charge densities for $N = 7, 11$ are displayed.

Note that $\delta E_2/\langle E_2\rangle$ also deviates from the RMT value of ≈ 0.52. This indicates that even for a chaotic geometry *the SCHF single-particle states near the Fermi level in the strong interaction regime no longer follow RMT due to charge rearrangement near the edge.*

The reorganized charge states at the edge differ from a two-dimensional Wigner crystal where the electrons are localized due to electron correlation energy [20].

One can distinguish two types of ordered states: For *smaller N* a phase which might be called a "crystal chain" evolves where the electrons are localized near the edge with clear spatial separation [see, e.g., Fig. 4(d)]. Because of quantum fluctuations of such a 1D crystal lattice this phase will be bounded from above by some critical electron number N_c. Since the minimum distance between the electrons should be larger than a Fermi wavelength λ_F, the maximum number of electrons which can reside at the edge is $\approx L_p/\lambda_F$, where L_p is the perimeter of the dot. Since in the crystal chain state all electrons are at the edge, N_c can be estimated as $N_c \approx L_p^2/A$, where we used $\lambda_F \approx R/\sqrt{N}$. For the dot geometries used we find N_c to be of the order of 10. This rough estimation is in line with our numerical results where for $N = 7$ all electrons are near the edge, whereas for $N = 11$ only 10 electrons seem close to the edge with one electron near the center of the dot [see Fig. 4(f)].

For the *larger* electron number $N > N_c$, as in Fig. 4(f), the charge density exhibits a modulation close to the edge rather than well-separated charges. Such ordered, charge-density-wave-like structures [21] persist up to high electron numbers. We still found these states for $N = 40$, the highest N considered. They play the same role for the enhancement of $\delta\chi$ (see, e.g., Fig. 3 for $N = 24$) as the crystal-type states do for $N < N_c$.

A few further remarks are due:

(i) A strongly deformed quantum dot where part of the boundary is concave [22] (insets of Fig. 2), renders the formation of edge states more difficult than the dot with a shape close to a disk due to the interplay between the long-range interaction and geometry. This is the reason why the fluctuations $\delta\chi$ are the largest in the latter case and turn out to be system dependent, even if the noninteracting geometries all exhibit chaotic dynamics.

(ii) The accumulation of charge near the edge alone is not sufficient to produce enhanced fluctuations $\delta\chi$, as visible in Figs. 4(c) and 4(e) for weakly interacting dots ($R/a_B^* = 5$). This weak interacting case, where $\delta\chi$ is still similar to the RMT value, can be understood within the RPA approach of Ref. [15], where the corresponding contribution to $\delta\chi$ was shown to be of the order of Δ or smaller, independent of the interaction strength. The formation of ordered states, which no longer follow RMT predictions, is necessary to generate enhanced fluctuations.

(iii) The shape dependence of the capacitive energy fluctuations found within our model, which does not include effects, e.g., from the dot surroundings, temperature, and spin, may be considered as one possible mechanism which can lead to the different widths in the peak spacing distributions of the various experiments [6–9].

An experimental observation of the interaction-dependent crossover of $\delta\chi$ would be particularly interesting. For GaAs samples with $a_B^* \approx 10$ nm, the crossover may appear for a system size close to 0.1 μm. Recent experiments [23] on small quantum dots without spatial symmetry may be a good testing ground.

In conclusion, we considered interaction effects in clean chaotic quantum dots. We propose as a mechanism for enhanced capacitive energy fluctuations, the formation of ordered charge states near the quantum dot edges. In the regime where the ordered states are developed the fluctuations are geometry dependent, even for chaotic systems.

We thank R. Berkovits, H. Castella, A. Cohen, Y. Gefen, S. Kettemann, A. D. Mirlin, G. Montambaux, and J.-L. Pichard for helpful discussions. K. H. A. thanks M. Takahashi for useful comments on numerical calculations.

[1] For a recent collection of papers see, e.g., special edition of Ann. Phys. (Leipzig) **7** (5-6) (1998).
[2] M. Stopa, Physica (Amsterdam) **251B**, 228 (1998).
[3] D. Ullmo, H. U. Baranger, K. Richter, F. von Oppen, and R. A. Jalabert, Phys. Rev. Lett. **80**, 895 (1998).
[4] *Chaos and Quantum Physics*, edited by M. J. Giannoni, A. Voros, and J. Zinn-Justin (North-Holland, New York, 1991).
[5] M. A. Kastner, Rev. Mod. Phys. **64**, 849 (1992).
[6] U. Sivan *et al.*, Phys. Rev. Lett. **77**, 1123 (1996).
[7] F. Simmel *et al.*, Europhys. Lett. **38**, 123 (1997).
[8] S. R. Patel *et al.*, Phys. Rev. Lett. **80**, 4522 (1998).
[9] F. Simmel *et al.*, Phys. Rev. B **59**, R10 441 (1999).
[10] A. Cohen *et al.*, Phys. Rev. B **60**, 2536 (1999).
[11] S. Levit and D. Orgad, Phys. Rev. B **60**, 5549 (1999).
[12] L. Bonci and R. Berkovits, cond-mat/9901332.
[13] P. N. Walker *et al.*, Phys. Rev. Lett. **82**, 5329 (1999).
[14] R. O. Vallejos *et al.*, Phys. Rev. Lett. **81**, 677 (1998).
[15] Y. M. Blanter *et al.*,Phys. Rev. Lett. **78**, 2449 (1997).
[16] R. Berkovits and B. L. Altshuler, Phys. Rev. B **55**, 5297 (1997).
[17] M. V. Berry and M. Robnik, J. Phys. A **19**, 649 (1986).
[18] H. Bruus and A. D. Stone, Phys. Rev. B **50**, 18 275 (1994).
[19] K.-H. Ahn and K. Richter, Physica E (to be published); Ann. Physik (Leipzig) (to be published).
[20] A. A. Koulakov and B. I. Shklovskii, Phys. Rev. B **57**, 2352 (1998).
[21] K. Hirose and N. S. Wingreen, Phys. Rev. B **59**, 4604 (1999).
[22] The shape sensitivity of the fluctuations $\delta\chi$ is not specific to the "kink" in the structure shown in the bottom right inset of Fig. 2, but also exists in deformed geometries with smooth confinement.
[23] D. G. Austing *et. al.*, cond-mat/9905135; S. Tarucha (private communication).